Contents lists available at ScienceDirect

Electrochimica Acta

journal homepage: www.elsevier.com

Enhanced performances of sensors based on screen printed electrodes modified with nanosized NiO particles

Marilena Carbone*, Alessia Nesticò, Noemi Bellucci, Laura Micheli*, Giuseppe Palleschi

Department of Chemical Sciences and Technologies, University of Rome Tor Vergata, Via della Ricerca Scientifica 1 00133, Rome, Italy

ARTICLE INFO

Article history:
Received 20 March 2017
Received in revised form 10 June 2017
Accepted 14 June 2017
Available online xxx

Keywords:
SPE NiO nanoparticle
peaks resolution

ABSTRACT

In this paper screen printed electrodes modified with NiO nanoparticles were developed and characterized. NiO nanoparticles were purposely synthesized by a microwave-assisted procedure followed by calcination either at 400 °C or 600 °C and characterized by X-ray diffraction and Scanning Electron Microscopy.

Screen printed electrodes were modified by drop casting either set of NiO nanoparticles dispersed in different solvents, i.e. H_2O, CH_3CN, ethanol and DMF-H_2O and characterized by Cyclic Voltammentry using ferrycianide as electroactive probe. All NiO-SPEs show enhanced performances with respect to the bare electrodes. The largest electroactive area, homogeneity, electron kinetic transfer and smallest peak-to-peak separation is displayed by the screen printed electrodes modified with NiO prepared at 400 °C and dispersed in H_2O. Thus this electrode was probed for the detection of benzoquinone, epinephrine and norepinephrine, demonstrating an enhancement of the electrochemical activity and a separation of the reduction peaks compared to the bare electrodes.

1. Introduction

The screen-printing technology is among the most powerful tools to underpin the progressive drive towards miniaturized, portable, sensitive devices [1,2]. The advantages of a single-use disposable sensor include the elimination of the problems associated with carryover of contamination or biofouling and the versatility of the design due to the ease of the surface modification by coating with different nanomaterials [3]. This allowed the assembling of cost-effective screen printed electrodes modified with nanoparticles of different type, morphology and size, which provide enhanced performances in the detection of selected targets.

Several types of nanoparticles have been used for coating: metals such as Au, Bi, Hg [4–7], or carbon materials [8–10], or nanoparticles-based composites and alloys [11–14]. Among them, some carbon materials have been depicted as particularly promising for building cost-effective sensors devices, since they show good conductivity, electrochemical stability, and long life cycle, but the energy density of carbon-based electrical double layer is limited by the electrostatic surface ion-adsorption charging mechanism [15,16]. Alternative inexpensive electrode materials with good capacitive characteristic are metal oxides such as NiO [17], CoO [18], MnO_2 [19,20], CuO [21–23], SnO_2 [24], and Fe_3O_4 [25]. Among oxides, NiO has attracted considerable attention for its lower cost, environment-friendly and high pseudocapacitive behavior and because of its properties it is applied in catalysis [26], electrochromic films [27], fuel cell electrodes [28], gas sensors [29]. NiO nanoparticles as enhancer of the electrodes performances are starting being explored with carbon paste electrodes, as shown by Aydoğdu et al. who found that NADH could be detected in the range from $1.0 \times 9\ 10^{-4}$ to 1.0 mmol L^{-1} with lower detection limit (0.05 μmol L^{-1}), when using NiO modified electrodes under optimum conditions [30]. NiO films have been deposited on screen printed electrodes for p-type dye-sensitized solar cells, showing an increased conductivity in the pristine status [31]. Films derived from NiO microballs, were used to modify screen printed electrodes to obtain efficient water oxidation catalysts [32]. Composites of NiO nanoparticles and multi-walled carbon nanotubes have been used to modify screen printed electrode for the electrooxidation of urea [33].

Due to the easy-to-use and versatility characteristics of SPEs, here we probed the performances enhancements of SPEs as sensors by modifications with NiO nanoparticles. As NiO properties are known to be morphology dependent [34–36], a suited synthesis was performed, via $Ni(OH)_2$ precursor obtained by a microwave assisted procedure followed by the calcinations at two different temperatures: 400 °C and 600 °C in air. The latter parameter appears to have a crucial role in the morphology of the NiO nanoparticles (NPs), along with the synthesis pathway and type of reagents used. This reflects in the electrochemical behavior, as shown in a recent paper of the group, where optical and electrochemical properties of the NiO nanoparticles have been correlated to their morphology [36]. In the present case, a microwave assisted synthesis with nickel acetate and ammonia was purposely tuned to achieve smaller nanoparticles. The outcome are NiO-NPs in the of on average 8 nm organized in agglomerated of 20–40 nm for the calcination at 400 °C and temperature, and 20–60 nm for the calcination at 600 °C. Such small and controlled nanoparticles allow a further rearrangement during the subsequent SPEs modification which was achieved by drop casting of the

* Corresponding authors. Tel.:+ +39 06 72594420; fax: +39 06 72594328, Tel: +39 06 72594470; fax: +39 06 72594328.
Email addresses: carbone@uniroma2.it (M. Carbone); laura.micheli@uniroma2.it (L. Micheli)

http://dx.doi.org/10.1016/j.electacta.2017.06.074
0013-4686/

synthesized NiO using different dispersing solvents, whose effects were evaluated in terms of transfer kinetics and electroactive area (the full characterization of the SPEs modified with NiO NPs dispersed H_2O is reported). The sensor showing the best electroanalytical performances was, then, tested for the detection of epinephrine, norepinephrine, and benzoquinone in order to highlight its electrochemical performances.

Epinephrine is a catecholamine with functions of hormone and inhibitory neurotransmitters in the message transfer in biology. Abnormalities of the epinephrine level are symptoms of several diseases, including Parkinsonism [37]. Furthermore, epinephrine drugs are also used to treat severe cases of bronchial asthma, anaphylactic shock, and organic heart disease [38]. Norepinephrine is also a catecholamine with multiple roles including hormone and neurotransmitter [39] that mediates chemical communication in the sympathetic nervous system [40,41]. The level of norepinephrine is important for monitoring and diagnosing diseases [42,43].

Benzoquinones, possessing two α,β-unsaturated carbonyl groups in a six-carbon atom ring, represent a uniquely important synthetic unit, such as in the synthesis of supramolecular dimeric structures [44], it is used as component of a flow battery [45], and is a product of oxidation of phenols in wastewaters [46]. Furthermore, the benzoquinone/benzoquinone$^{\cdot-}$ redox couple can be used for testing a large number of reactions, such as liquid junction photoelectrochemical solar cells [47].

The exploitation of devices for sensitive point-of-care and reliable quantification of epinephrine, norepinephrine and benzoquinone has become increasingly important and different strategies have been reported for their analysis [48–55].

To our knowledge, up to now no screen printed sensors based on NiO has been reported for detection of norepinephrine, epinephrine and benzoquinone. Thus, screen-printed carbon electrodes were modified with easily prepared NiO-NPs, and achieved good sensitivities for all tested compound, leading to development of a cheap and simple device.

2. Experimental

2.1. Reagents

Analytical grade nickel(II)acetate ($Ni(CH_3CO_2)_2$ *$4H_2O$, 98%,Aldrich), ammonia, KCl, ethanol, DMF, acetonitrile (CH_3CN), $K_3[Fe(CN)_6]$, epinephrine, norepinephrine, NADH and benzoquinone were purchased from Sigma-Aldrich (Milan, Italy). Phosphate-buffered saline (PBS, 0.1 M, Na_2HPO_4-NaH_2PO_4-KCl, pH 7.4) was prepared from a PBS tablet (Sigma, USA) with deionized water.

2.2. Apparatuses

X-ray diffraction (XRD) patterns of the synthesized samples were collected with an expert pro x-ray diffractometer by Philip, using CuK-Alpha radiation. Scanning Electron micrographs (SEMs) of the oxides as well as of the modified electrodes were collected with a Zeiss Auriga Field Emission-Scanning Electron Microscope instrument operating at 6–8 kV

Electrochemical measurements were performed at room temperature, using a computer-controlled system, AUTOLAB model GPSTAT-12 with GPES software, (Ecochemie, Utrecht, The Netherlands). Screen-printed electrodes (SPEs) used for CV were made by precision screen printer DEK 245 (DEK, Weymouth, UK). Inks were from Acheson Italia (Milan, Italy). The resulting SPE, which consists of a graphite working electrode, a silver pseudo-reference electrode, and a graphite counter electrode, forms a complete electrochemical cell. The diameter of the working electrode was 0.3 cm, which resulted in an apparent geometric area of 0.07 cm^2. Cyclic voltammograms (CVs) were recorded in potential range between −1 and 1 V at different scan rates.

2.3. NiO-NPs Synthesis

The synthesis of $Ni(OH)_2$ was carried on using analytical grade nickel(II)acetate ($Ni(CH_3CO_2)_2$ * $4H_2O$) and ammonia. In a typical synthesis, 0.0174 mol of $Ni(CH_3CO_2)_2$ were dissolved in 83 mL of deionized water under magnetic stirring at room temperature till complete dissolution. Ammonia solution (17 mL, 33%) was added and the stirring was carried on for 3 h. The resulting mixture was transferred to a conventional microwave oven (MARS model, CEM, Italy) operated at 62% of the maximum power (1600W), 2450 MHz, and was heated at 145 °C for 10 min by microwave irradiation. The mixture was, hen, cooled to room temperature and filtered. The resulting powder was repeatedly washed with deionized water and dried at 80 °C prior to the XRD analysis. Afterwards, quotas of the powder precursor were place in a tubular oven and heated up at a rate of 10°/min till the target temperature was reached. Calcinations were, then, carried out at 400 °C or at 600 °C for 3 h in air atmosphere.

2.4. Modification of the SPEs

The following procedure was adopted to produce the sensing electrodes modified with NiO (NiO-SPE). Typically 1 mg NiO was dispersed in 1 mL of the chosen solvent (H_2O, CH_3CN, EtOH or DMF/H_2O 1:1 v/v). After 1 h sonication of the dispersion at 59 Hz and room temperature, quotas of 6 μL of were deposited on the surface of the working electrodes. The evaporation of the solvent on the electrode surface was achieved within a moist chamber at 25 °C and finally the electrodes were ready for analysis. Prior to the modification of the electrodes, the SPEs were pre-treated in PBS 0.01 M, 0.1 M KCl, pH 7.4, by applying an anodic potential of 1.7 V for 180 s. They were, then, stored dry at room temperature, in the dark, ready to use. All the modified NiO-SPEs were prepared in triple.

3. Results and Discussion

3.1. Structural analysis

XRD and SEM were employed to gather phase and structural information of both the precursor and the calcined samples. Fig. 1a) shows the XRD pattern of the precursor obtained by microwave assisted synthesis. All the diffraction peaks can readily be indexed to the hexagonal α-$Ni(OH)_2$, phase [56]; consequently the reflections at 2θ = 19.4, 33.3, 38.7, 52.2, 59.2, 60.2, 62.9, 69.6 and 70.5 have been assigned to the (001), (100), (011), (012), (110) (003) (111) (200) (103) planes, respectively. Neither a peaks' shift is observed, nor are secondary peaks present, indicating that there are no spurious phases or contaminations. The XRD patterns of the calcined samples are reported in Fig. 1b) and both correspond to a NiO phase [57], without any contamination. Therefore, the peaks at 2θ = 37.4, 43.4, 63.0, 75.5, 79.6 have, been assigned to the (111), (200), (220), (222) and (311) reflections, respectively.

The different calcination temperatures had an effect on the mean size of the NiO crystallites as can be deduced by the different FWHM of the diffraction peaks of the two samples. By applying the Debye formula to the (200) reflection (see the Supplementary information), the average diameter of the nanoparticles of NiO calcined at 400° (NiO400 °C) is estimated to be 8 nm, whereas the nanoparticles of NiO calcined at 600 °C (NiO600 °C) have an estimated average diameter of 30 nm.

The different NiO crystallite size and morphology can also be appreciated in the SE micrographs reported in Fig. 2 at two magnifica-

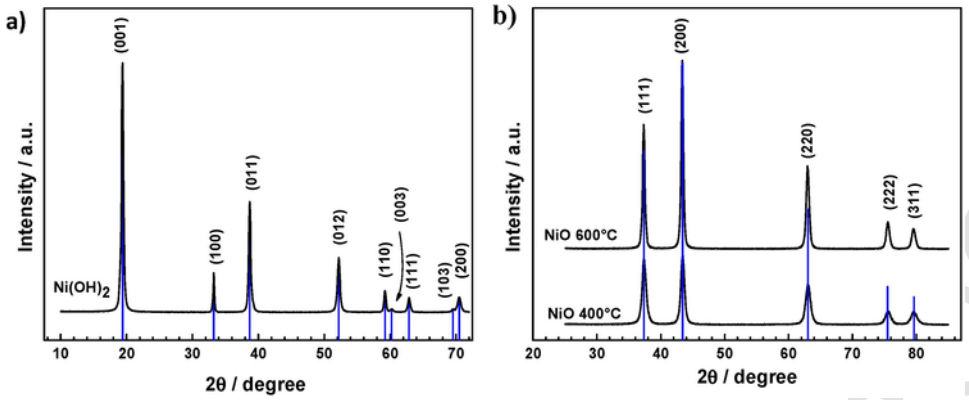

Fig. 1. a) XRD pattern of the synthesized $Ni(OH)_2$ (black solid line) compared to the reference data [53] (vertical blue lines). **b)** XRD patterns of the NiO samples (black solid lines), compared to the reference data (vertical blue lines) [54], bottom: NiO400 °C, top: NiO600 °C.

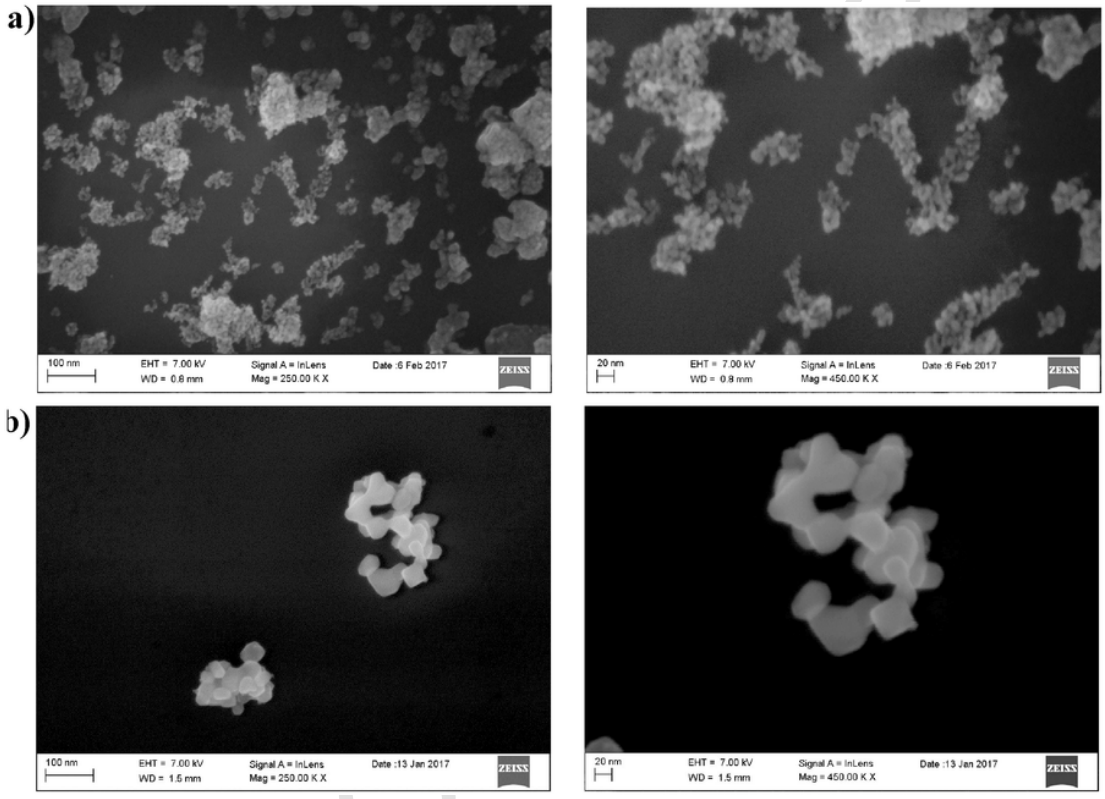

Fig. 2. SE micrographs of a) NiO–400 °C and b) NiO–600 °C samples: left panels 250Kx magnification, right panels 450Kx magnification.

tions. The preparation at 400 °C is characterized by nanosized NiO particles in the 8 nm range arranged in agglomerates of 20–60 nm. The nanoparticles obtained at 600 °C are in the 20–40 nm range and do not present any finer granular structure.

3.2. Surface characterization of the modified electrodes

The electrochemical properties of electrodes modified with nanomaterials largely depend on the nanoparticles morphology. Shape-dependency of the nanoparticles electroactivity has been reported in several studies such as the electrocatalysis of glucose oxidation using gold nanoparticles, [58] or the transfer kinetics and catalytic activity of NiO nanoparticles for glucose sensors [59]. In addition, the drop casting procedure may induce morphological effects on the nanoparticles, depending on the solvents properties, such as the polarity [60]. Therefore, the surface morphology of the SPEs modified with NiO-NPs was characterized by SEM, and the corresponding measurements are reported in Fig. 3. Upon drop-casting on SPEs and voltammetric cycling the NiO-NPs partially re-aggregate, the size, size dispersion, texture and shape of the aggregates, depending on the NiO-NPs size and the dispersing solvent. The morphology of the different modified electrodes is, then, associated to the electroactive areas and sensitivities, calculated as explained in the following section. The dispersion in H_2O, i.e. the solvent with the highest dielectric constant, affords the most regularly shaped aggregates, mostly roundish, with a diameter of 100–140 nm if derived from the 400 °C NPs and a diameter of 160-210 if derived from the 600 °C NPs. Although the shape in both cases is similar, the difference in size of the nanoparticles is responsi-

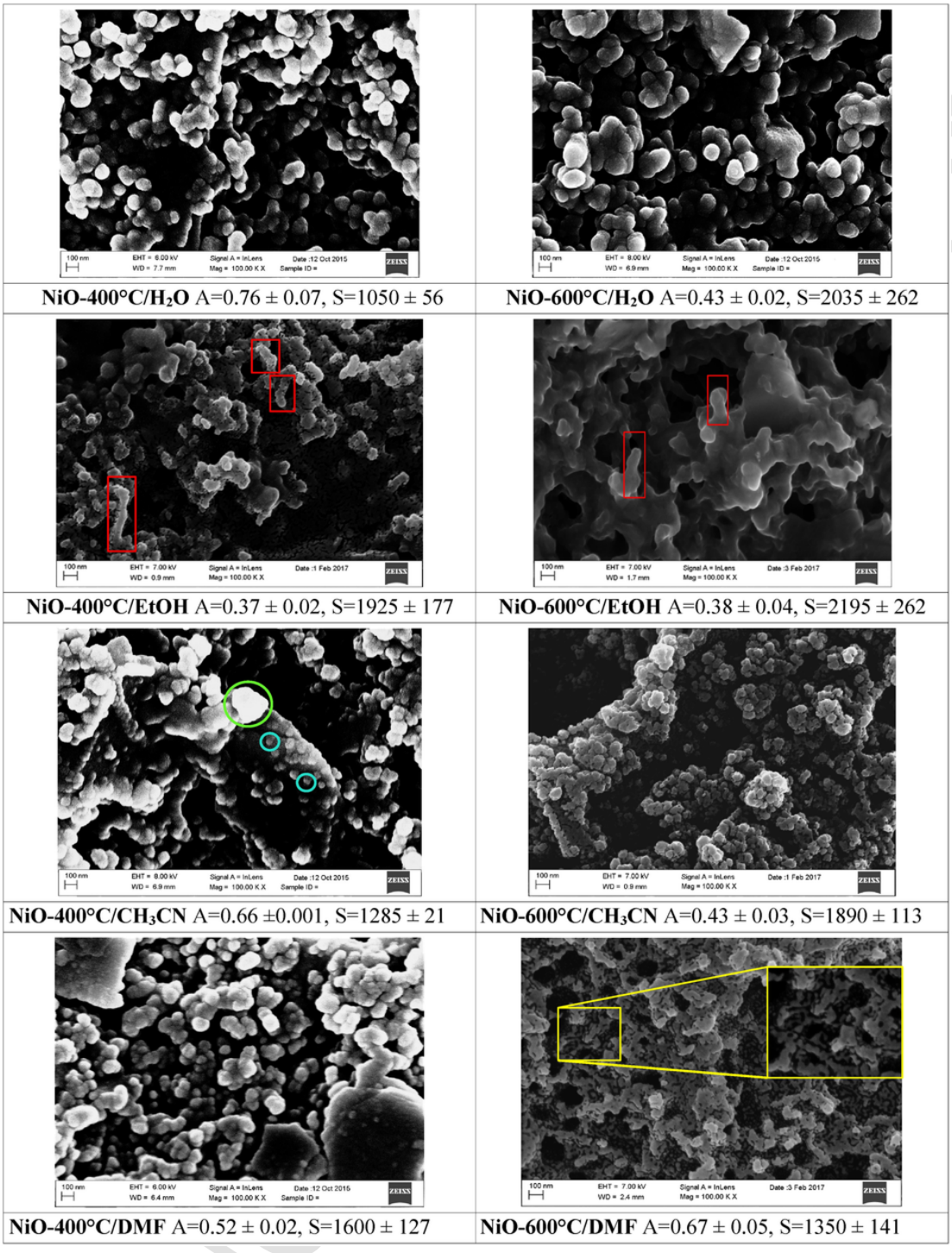

Fig. 3. SE micrographs of the NiO modified SPEs at 100 000 x magnifications. The type of NiO preparation and the dispersing solvents are reported under each micrograph, along with the electroactive area (A) and the sensitivity (S).

ble for significantly different electroactive areas, i.e. 0.76 ± 0.07 nm^2 (the highest of all) for the former and 0.43 ± 0.02 nm^2 (among the lowest) for the latter. The drop casting of NiO from ethanol dispersion results in aggregates of rather elongated shapes, as highlighted in the red rectangles of Fig. 3, with the long axis which can vary between 100 and 400 nm (red rectangles). These shapes correspond to the lowest electroactive areas and the highest sensitivities of the whole set of modified electrodes, with no significant difference between the 400 °C and 600 °C preparations. The morphologies resulting from the dispersions of the NiO-NPs from CH_3CN and from the mixture of DFM-H_2O are more irregular in shape and size distribution. The re-aggregation of NiO400 °C-NPs from the CH_3CN dispersion is only partial and this results in the simultaneous presence of smaller nanoparticles (~10 nm, light blue circles) and larger aggregates (~200 nm, green circles). The re-aggregation of the

NiO600 °C-NPs from the CH_3CN dispersion affords particles with a more homogeneous size, i.e. 80–100 nm, organized in larger agglomerates. The combination of size and size distribution gives an overall larger surface for the former, associated to a lower sensitivity.

Opposite trend of electroactive areas is found for the re-aggregations of NiO400 °C-NPs and NiO600 °C-NPs when using DMF-H_2O solvents. The re-aggregation is mostly regular for both NiO preparations, but with the appearance of occasional large aggregates in the former one In addition, the 600 °C re-aggregation presents a sort of granular network structure (see inset in the yellow frame). This leads to some differences in electroactive areas and sensitivity between the two preparations, at variance with the previous case.

3.3. Electrochemical characterization

The electrochemical sensing properties of the different NiO modified electrodes were first examined using $[Fe(CN)_6]^{3-/4-}$. Eight sets of measurements were performed, i.e. one for each combination of NiO preparation and solvent. A pair of redox peaks is observed in the voltammograms of the modified SPEs, with a peak-to-peak potential separation smaller than that of the bare electrodes. They also show increased anodic and cathodic peak intensities, thus implying that the electron transfer at the solution/electrode interface is fast due NiO-related enhanced conductivity (in agreement with the literature data [61]). Tables SI1a and b report the anodic and cathodic peak current, the peak-to-peak separation (E_{pa}-E_{pc} = ΔEp), the anodic and cathodic peak intensities, in 50 mM phosphate buffer (pH 7.4), 0.1 M KCl, and 20 mM of redox probe.The ΔE_p values of the NiO modified SPEs varies both with the type of NiO preparation and with the solvent used as dispersing agent. The smallest and second smallest ΔE_p are obtained using H_2O as solvent and NiO400 °C-NPs (ΔE_p = 173 ± 9 mV) NiO600 °C-NPs (ΔE_p 186 ± 38 mV), respectively, followed NiO400 °C-NPs dispersed with EtOH (214 ± 10 mV) and NiO600 °C-NPs dispersed in DMF-H_2O (229 ± 19 mV). All the other modifies SPEs have ΔE_ps in the 250 mV range.

To elucidate the origin of the enhancement effects of the signals, the effective surface area of the NiO-SPEs was determined from the voltammetric peak current using the Randles-Sevcik equation (Eq. (1), [62])

$$I_p = 0.4463nFAC\sqrt{\frac{nFvD}{RT}} \quad (1)$$

where I_p is the intensity of current peak (A), A is the electrode surface area (cm^2), v is the scan rate (V/s), n the number of electrons involved in the redox reaction, F is the Faraday constant (C_*mol^{-1}), T is the Kelvin temperature (K), R is the universal gas constant (8.314 J/mol$_*$K), D is the diffusion coefficient of the molecule in solution (7.26 10^{-6} cm^2s^{-1} for ferrycianide ([63]) C is the concentration of the redox species in solution (mol cm^{-3}) and m is the slope of the linear fit (y = mx + q) of the peak current *vs.* $v^{1/2}$ (Eq. (2)) calculated as follows:

$$m = \cos t = nFAC\sqrt{\frac{nFvD}{RT}} \quad (2)$$

According to Eq. (1), the peak current is directly proportional to the concentration of the analyte in bulk solution and increases with the square root of the scan rate.

In Fig. 4 a) through c) CVs are reported of bare SPE and SPE modified with NiO400 °C and dispersed in H_2O at various scan rates along with the corresponding plot of the anodic and cathodic peak current *vs.* $v^{1/2}$.

A linear trend was observed between the anodic and cathodic peak intensity and the square root of the potential scan rate in the − 1 and 1 V/s range, indicating a diffusion-controlled process the electrodes [64]. Furthermore, the increased slope of the I_p *vs* $v^{1/2}$ plots, as compared to the bare electrodes indicates a significant enhancement of the total electroactive area. The CVs as a function of the scan rate were, then, repeated for all NiO dispersions the effective surface areas and sensitivity calculated and the results reported in Fig. 3 associated to the micrographs of the corresponding modified SPEs and summarized in Table SI2. Briefly, the largest electroactive surface

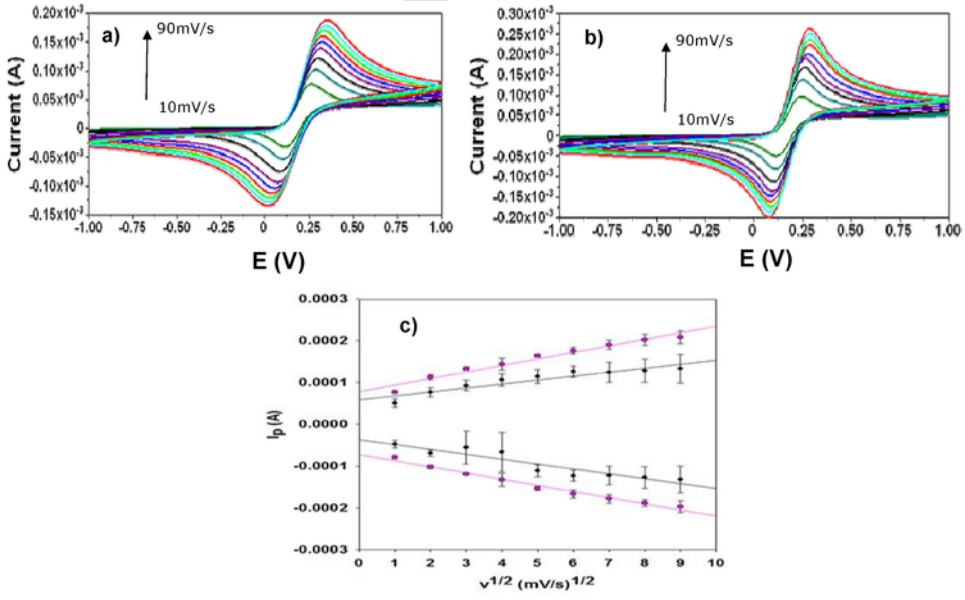

Fig. 4. a) CVs of bare SPE and **b)** CVs of SPE modified with NiO400 °C dispersed in H_2O at various scan rates: 10, 20, 30, 40, 50, 60, 70, 80, 90 mV/s) in 50 mM phosphate buffer, 0.1 M KCl, pH 7.4. **c)** Anodic and cathodic peak current vs. $v^{1/2}$ of bare SPE (●), and SPE modified NiO (●).

area is achieved with the NiO400 °C dispersed in H_2O, the highest sensitivity with NiO600 °C also dispersed in H_2O.

The measurements were repeated 10 times for each modified SPE and the best reproducibility was achieved with the NiO400 °C-NPs dispersed in H_2O (RSD% 6).

According to the CV results, NiO nanoparticles facilitate the electron transfer between the redox probe solution and the surface of the modified electrode due to a high electroactive surface area and the electric conductivity of NiO nanoparticles.

Using these results and the Nicholson equation:

$$k_s = \frac{\left(D_o \cdot \frac{nF}{RT} \cdot \pi \cdot v\right)^{1/2}}{\left(D_o/D_r\right)^{\alpha/2}} \cdot \Psi \quad (3)$$

the electrode surface related electron transfer coefficients (K_s) were calculated for the whole set of the modified NiO-SPEs, the faster electrode transfer attaining to the SPE modified with NiO400 °C-NPs dispersed in H_2O (K_s 1.63×10^{-3}) [65]. In Eq. (3) D_0 and D_r are the diffusion coefficients of $[Fe(CN)_6]^{3-}$ and $[Fe(CN)_6]^{4-}$, respectively as reported by Konopka and McDuffie [63], v is the scan rate (V/s), α is a transfer coefficient, usually approximated to 0.5 for reversible processes, ψ a transfer parameter related to the ΔEp.

The best performance in terms of reproducibility, ΔEp, electrode transfer and electroactive surface area was given by SPE modified by with NiO400 °C-NPs dispersed in H_2O. Therefore, this type of electrode was used for further investigations of NiO-NPs load effects and electrochemical determination of norepinephrine, epinephrine and benzoquinone.

3.4. The effect of NiO-NPs load on the performance of the NiO-SPEs

The influence of the loading of the NiO-NPs on the electrode surface was determined by examining the voltammetric response. Fig. SI2 shows the cyclic voltammograms obtained by drop casting NiO400/H_2O dispersions with ratios 0.5, 1.0 or 1.5 mg mL^{-1}. The increase of the loading from 0.5 to 1.0 mg mL^{-1} leads to sharper peaks with smaller peak separation (173 mV), suggesting an increase in electrochemical reversibility. The further increase of the load to 1.5 mg mL^{-1} results in an excessive nanoparticle deposition that could disturb the electron transfer on the electrode surface, similarly to findings reported by Qu et al. [66] and Chairam et al. [67]. The electrochemical characteristics of the SPEs modified at different loadings are reported in Table 2. can be noticed that the 1.0 mg mL^{-1} electrode, besides the smallest ΔE_p also displays lowest the RSD%. Finally the 1.0 mg mL^{-1} electrode was probed for operational and room temperature storage stability, by running 20 successive CVs of ferrycianide (RSD% < 1.5) and by repeating the 5 CVs every week for three months (which causes an increase of the RSD up to 5%) (Table 1).

Table 1
Comparison of electrochemical characteristic of modified SPEs at different loads at NiO400° dispersed in H_2O (see Fig. SI1).

Load	E_{pa} (mV)	E_{pc} (mV)	ΔE_p (mV)	RSD%	i_{pa} (μA)	i_{pc} (μA)
0.5 mg/ml	323 ± 24	37 ± 12	284 ± 18	10	150 ± 17	−144 ± 18
1.0 mg/ml	288 ± 6	116 ± 12	173 ± 9	6	164 ± 3	−153 ± 5
1.5 mg/ml	303 ±15	61 ± 8	242 ± 12	9	155 ± 8	−152 ± 14

3.5. Cyclic Voltammetries of benzoquinone, norepinephrine and epinephrine at NiO400 °C/$H_2$0 modified SPEs

To get further insight into its electroanalytical performance, the NiO400 °C-SPE/H_2O was used for the study of the electrochemistry of benzoquinone, epinephrine and norepinephrine and the results compared to the bare SPEs. All the analytes in Fig. 5 indicate a clear reversibility, a decrease of the peak-to-peak separation and an enhanced electrochemical reactivity with a two to sevenfold increase of the cathodic and anodic peaks intensity with respect to the corresponding bare electrodes (see Table 2).

The redox processes of benzoquinone, norepinephrine and epinephrine are 2 electrons and two protons one as sketched in Fig. 5 d). In addition to the enhanced electrocatalytic performances, the NiO400 °C/H_2O SPE has the capability of resolving the single redox steps, the correspondence between redox reactions and peaks intensity having been highlighted in Fig. 5. Only benzoquinone has single anodic peak, though the two clearly distinct peaks can be singled out in the cathodic wave.

The modification of SPEs by drop casting of nanomaterials for the detection norepinephrine, epinephrine and benzoquinone was investigated by using carbon-black (benzoquinone and epinephrine) [68], graphene oxide (epinephrine and norepinephrine) [69], graphene oxide mixed with ionic liquids (epinephrine and norepinephrine) [70], and nanohorns [71] (epinephrine). In all these cases, the modified electrodes indicated an enhanced electrochemical effect as compared to the bare electrodes, along with a peak-to-peak separation decrease. In none of those cases, however the single redox steps could be resolved. The observed cathodic/anodic peaks, therefore, either indicate that both electrons are transferred in a single step or that only one redox step is observed, the second having a much higher overpotential. The capability of resolving the redox peaks in the case of NiO400 °C/H_2O electrode gives the opportunity of selecting a single redox step for the analyte detection, with the option a setting a narrower potential window.

4. Conclusions

Low-cost, environment-friendly easy-to-fabricate, screen-printed electrodes modified with NiO NPs were developed and characterized. NiO NPs were purposely synthesized via a microwave assisted procedure followed by calcination at 400 °C and 600 °C, and the best con-

Table 2
Summery of the electrochemical parameters and of the concentration of the analytes. EP = epinephrine, NE = norepinephrine, BQ = benzoquinone. The subscript I refers to the first redox step, II to the second one as indicated in Fig. 5.

Analyte	Electrode	Conc. *(mM)*	E_{pcI} *(mV)*	E_{paI} *(mV)*	ΔE_I *(mV)*	i_{pcI} *(μA)*	i_{paI} *(μA)*	E_{pcII} *(mV)*	E_{paII} *(mV)*	ΔE_{II} *(mV)*	i_{pcII} *(μA)*	i_{paII} *(μA)*
EP	NiO400/H_2O	5	123	−219	***96***	24	−49	417	245	***172***	91	−20
	Bare	5	−101	−279	***178***	6	−19	477	268	***209***	37	−10
NE	NiO400/H_2O	5	−140	−204	***64***	2	−12	360	116	***244***	25	−8
	Bare	5		−215			−6	383	105	***278***	11	−4
q	NiO400/H_2O	1	−114			20	−38	131	−232	***363***	18	−26
	Bare	1	−89			10	−17	163	−243	***406***	11	−17

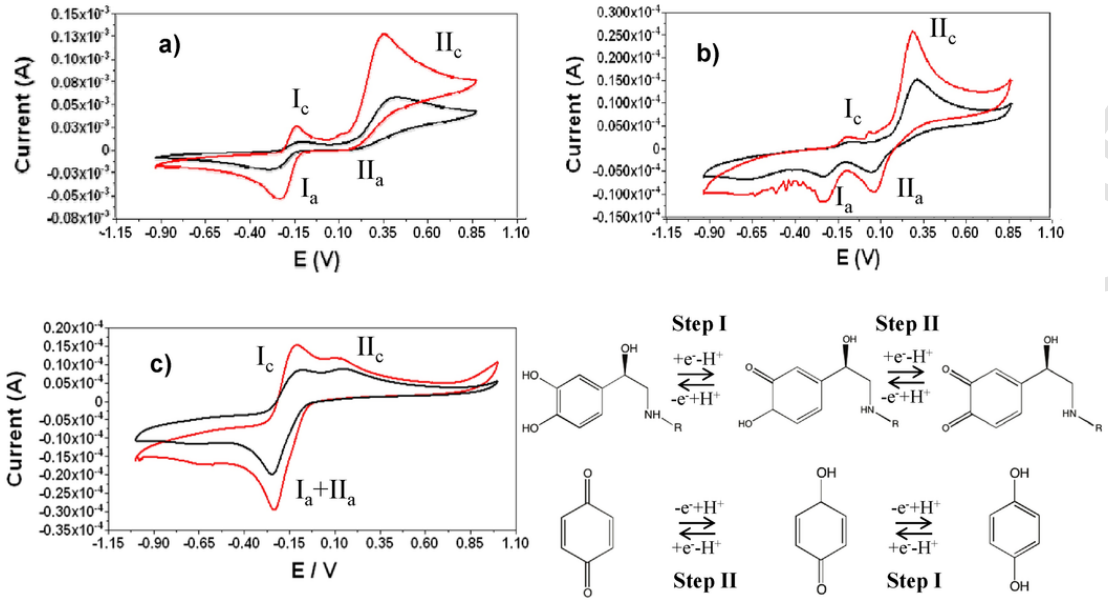

Fig. 5. CV using bare SPEs (black curves) or NiO400 °C/H_2O modified SPEs (red curves) for a) 5 mM epinephrine in 0.05 M acetate buffer, KCl 0.1 M, pH = 5, b) 5 mM norepinephrine in 0.05 M acetate buffer, 0.1 M KCl, pH = 5, and c) 1 mM benzoquinone in 0.05 M phosphate buffer, 0.1 M KCl, pH = 7.4. In panel d) the scheme of the two stepped redox reactions is reported. R = CH_3 for the epinephrine and R = H for the norepinephrine. The peaks marked with I refer to the first step of the redox reaction, those marked with II to the second one.

ditions for drop casting were explored by using different dispersing solvents, i.e. H_2O, CH_3CN, EtOH and DMF-H_2O. A partial re-aggregation of the NiO-NPs occurs upon drop casting and CV cycling, to an extent that depends on the NiO preparation and the dispersing agent. The SPE modified with NiO prepared at 400 °C and dispersed in H_2O has the largest electroactive area, the smallest peak-to-peak separation and the largest electron transfer kinetic constant of the whole set and was selected for the detection of epinephrine, norepinephrine and benzoquinone. The NiO modified SPE has a higher peaks intensity, a smaller peak-to-peak separation and a better resolution of the single redox steps as compared to the bare electrode, making this sensor a suitable tool for electrochemical applications. Compared to other nanoscale carbonaceous materials drop casted on SPEs, it has a better redox steps resolution, which allows a selection of a narrower potential window for the epinephrine and norepinephrine detection.

Acknowledgments

This research did not receive any specific grant from funding agencies in the public, commercial, or not-for-profit sectors.

Appendix A. Supplementary data

Supplementary data associated with this article can be found, in the online version, at http://dx.doi.org/10.1016/j.electacta.2017.06.074.

References

[1] K. Yamanaka, Mun'delanji C. Vestergaard, E. Tamiya, Sensors 1761 (2016) 1–16.
[2] J. Barton, M. Begoña, G. García, D. Hernández, S.P. Fanjul-Bolado, A. Ribotti, M. McCaul, D. Diamond, P. Magni, Microchim Acta 183 (2016) 503–517.
[3] A. Hayat, J.L. Marty, Sensors 14 (2014) 10432–10453.
[4] A. Mandil, L. Idrissi, A. Amine, Microchim. Acta 170 (2010) 299–305.
[5] R.A. Farghali, Rasha A. Ahmed, Int. J. Electrochem. Sci. 10 (2015) 1494–1505.
[6] B. Molinero-Abad, M.A. Alonso-Lomillo, O. Dominguez-Renedo, M.J. Arcos-Martinez, Microchim. Acta 180 (2013) 1351–1355.
[7] A. Samphao, P. Butmee, J. Jitcharoen, 1 Ľ, Ľ. Švorc, G. Raber, K. Kalcher, Talanta 142 (2015) 35–42.
[8] M. Trojanowicz, Trend Anal. Chem. (2016) http://dx.doi.org/10.1016/j.trac.2016.03.027.
[9] S. Cinti, F. Arduini, M. Carbone, L. Sansone, I. Cacciotti, D. Moscone, G. Palleschi, Electroanal. 7 (2015) 1–10.
[10] F. Valentini, D. Roscioli, M. Carbone, V. Conte, B. Floris, E.M. Bauer, N. Ditaranto, L. Sabbatini, E. Caponetti, D. Chillura-Martino, Sensors Actuat. B-Chem 212 (2015) 248–255.
[11] P. Niu, C. Fernández-Sanchez, M. Gich, C. Navarro-Hernández, P. Fanjul-Bolado, A. Roig, Microchim. Acta 1 (183) (2016) 617–623.
[12] B. Derkus, E. Emregul, K.C. Emregul, Talanta 1 (134) (2015) 206–214.
[13] N. Lavanya, C. Sekar, S. Ficarra, E. Tellone, A. Bonavita, S.G. Leonardi, G. Neri, Mater. Sci. Eng. C 62 (2016) 53–60.
[14] M. Hjiri, R. Dhahri, N. Ben Mansour, L. El Mir, M. Bonyani, A. Mirzaei, S.G. Leonardi, G. Neri, Materials Letters 160 (2015) 452–455.
[15] E. Raimundo-Piñero, F. Leroux, F. Béguin, Materials Letters 18 (2006) 1877–1882.
[16] M.M. Shijumon, F.S. Ou, L.J. Ci, P.M. Ajayan, Chem. Commun. (2008) 2373–2375.
[17] J. Zhao, H. Liu, Q. Zhang, Appl. Sur. Sci. 392 (2017) 1097–1106.
[18] Y.-B. Liu, L.-Y. Lin, Y.-Y. Huang, C.-C. Tu, J. Power Sources 315 (2016) 23–34.
[19] P. Liu, N. Zhang, Z. Cheng, Y. Qiu, P. Xu, W. Huang, H. Fan, M. Zhang, F. Cheng, Ionics 23 (2017) 247–251.
[20] A.-M. Gurban, D. Burtan, L. Rotariu, C. Bala, Sensors Actuat. B 210 (2015) 273–280.
[21] S.C. Bhise, D.V. Awale, M.M. Vadiyar, S.K. Patil, B.N. Kokare, S.S. Kolekar, J. Solid State Electrochem. in press. 10.1007/s10008-016-3490-2.
[22] M. Carbone, J Alloy Compd. 688 (2016) 202–209.
[23] M. Carbone, R. Briancesco, L. Bonadonna, Environ. Nanotechnol. Monit. Manage. 7 (2017) 97–102.
[24] V. Bonu, B. Gupta, S. Chandra, A. Das, S. Dhara, A.K. Tyagi, Electrochim. Acta 203 (2016) 230–237.
[25] Y. Zeng, M. Yu, Y. Meng, P. Feng, X. Lu, Y. Tong, Adv. Energy Mater. 6 (24) (2016) 1601053.
[26] K. Hayat, M.A. Gondal, M.M. Khaled, S. Ahmed, J. Mol. Catal. A 336 (2011) 64–71.
[27] X.H. Xia, J.P. Tu, J. Zhang, X.L. Wang, W.K. Zhang, H. Huang, Electrochim. Acta 53 (2008) 5721–5724.
[28] B. Park, E.J. Cairns, Electrochem. Commun. 13 (2011) 75–77.
[29] H. Steinebach, S. Kannan, L. Rieth, F. Solzbacher, Sensor Actuat. B-Chem. 151 (2010) 162–168.

[30] G. Aydoğdu, D. Koyuncu Zeybek, B. Zeybek, S. Pekyardımcı, J. Appl. Electrochem. 43 (2013) 523–531.
[31] M. Bonomo, G. Naponiello, A. Di Carlo, D. Dini, Sci. Nanotechnol. 4 (2) (2016). 201-1/18.
[32] A. Singh, M. Fekete, T. Gegenbach, A.N. Simonov, R.K. Hocking, S.L.Y. Chang, M. Rothmann, S. Powar, D. Fu, Z. Hu, Q. Wu, Y.-B. Cheng, U. Bach, L. Spiccia, Chem. Suc Chem. 8 (2015) 4266–4274.
[33] E. Lohrasbi, M. Asgari, Adv. Anal. Chem 5 (3A) (2015) 9–18.
[34] Y. Yang, Y. Liang, Z. Zhang, Y. Zhang, H. Wu, Z. Hu, J. Alloys Compd 658 (2016) 621–628.
[35] D.S. Hall, D.J. Lockwood, C. Bock, B.R. MacDougall, 20140792 Proc. R. Soc. A 471 (2014) 1–65.
[36] M. Carbone, E.M. Bauer, L. Micheli, M. Missori, Colloid Surface A, in press, 10.1016/j.colsurfa.2017.05.046.
[37] M.A. Dayton, J.C. Brown, K.J. Stutts, R.M. Wightman, Anal. Chem. 52 (1980) 946–950.
[38] E.D. Bergmann, Z. Goldschmidt, J. Medicinal Chem. 11 (1968) 1121–1125.
[39] M. Cui, Y. Feng, D.J. McAdoo, W.D. Willis, J. Pharmacol. Exp. Ther. 289 (1999) 868–876.
[40] H. Zhao, Y. Zhang, Z. Yuan, Anal. Chim. Acta 454 (2002) 75–81.
[41] W. Ren, H.Q. Luo, N.B. Li, Biosens. Bioelectron. 21 (2006) 1086–1092.
[42] J.I. Friedman, D.N. Adler, K.L. Davis, Biol. Psychiatry 46 (1999) 1243–1252.
[43] D. Voet, J.G. Voet, Biochemistry, 2nd ed., Wiley, New York, 1995.
[44] M. Ishida, H. Fujimoto, T. Morimoto, S. Mori, M. Toganoh, S. Shimizu, H. Furuta, Supramol. Chem. 29 (2017) 8–16.
[45] P.K. Leung, T. Martin, A.A. Shah, M.R. Mohamed, M.A. Anderson, J. Palma, J. Power Sources 341 (2017) 36–45.
[46] N. Villota, J.M. Lomas, L.M. Camarero, Desalination Water Treat. 57 (59) (2016) 28784–28793.
[47] H.-Y. Hsu, L. Ji, M. Du, J. Zhao, E.T. Yu, A.J. Bard, Electrochim. Acta 220 (2016) 206–210.
[48] D.V. Chernyshov, N.V. Shvedene, E.R. Antipova, I.V. Pletnev, Anal. Chim. Acta 621 (2008) 178–184.
[49 B.J. Sanghavi, O.S. Wolfbeis, T. Hirsch, N.S. Swami, Microchim Acta 182 (2015) 1–41.
[50] A.R. Smith, P.A. Garris, J.M. Casto, J. Chem. Neuroanatomy 66–67 (2015) 28–39.
[51] S. Casadio, J.W. Lowdon, K. Betlem, J. Tadashi, C.W. Foster, T.J. Cleij, B. van Grinsven, O.B. Sutcliffe, C.E. Banks, M. Peeters, Chem. Eng. J. in press. 10.1016/j.cej.2017.0.
[52] I.M. Apetri, C. Diaconu, C. Apetri, C. Georgescu, Romanian Biotechnol. Lett. 21 (2016) 11092–11102.
[53] S.-H. Huang, H.-H. Liao, D.-H. Chen, Biosens. and Bioelectr. 25 (2010) 2351–2355.
[54] Y. Wang, S. Wang, L. Tao, Q. Min, J. Xiang, Q. Wang, J. Xie, Y. Yue, S. Wu, X. Li, H. Ding, Biosens. and Bioelectr. 65 (2015) 31–38.
[55] S. Korkut, S. Uzuncar, M.S. Kilic, B. Hazer, Instrument. Sci. and Technol. 44 (2016) 614–628.
[56] JCPDS 73-1520.
[57] JCPDS 22-1189.
[58] S. Karra, M. Wooten, W. Griffith, W. Gorski, Electrochim. Acta 218 (2016) 8–14.
[59] E. Sharifi, A. Salimi, E. Shams, A. Noorbakhsh, Biosens. Bioelectron. 56 (2014) 313–319.
[60] T.G. Dane, J.E. Bartenstein, B. Sironi, B.M. Mills, O.A. Bell, J.E. Macdonald, T. Arnold, C.F.J. Faul, W.H. Briscoe, Phys. Chem. Chem. Phys. 18 (2016) 24498–24505.
[61] F.-B. Zhang, Y.K. Zhou, Mater. Chem. Phys. 83 (2–3) (2004) 260–264.
[62] J. Wang, Anal electrochem, Wiley, Hoboken, 200629–66.
[63] S.J. Konopka, B. McDuffie, Anal. Chem. 42 (1970) 1741–1746.
[64] M.-J. Song, J. Kim, S. Lee, J.-H. Lee, D. Lim, S. Hwang, D. Whang, Microchim. Acta 171 (3–4) (2010) 249–255.
[65] R.S. Nicholson, Anal. Chem. 37 (1965) 1351–1355.
[66] S. Qu, J. Wang, J. Kong, P. Yang, G. Chen, Talanta 71 (2007) 1096–1102.
[67] S. Chairam, W. Sroysee, C. Boonchit, C. Kaewprom, T. Goedsak, N. Wangnoi, M. Amatatongchai, P. Jarujamrus, S. Tamaung, E. Somsook, J. Electrochem. Sci. 10 (2015) 4611–4625.
[68] F. Arduini, F. Di Nardo, A. Amine, L. Micheli, G. Palleschi, D. Moscone, Electroanal. 24 (4) (2012) 743–751.
[69] F. Valentini, D. Romanazzo, M. Carbone, G. Palleschi, Electroanal. 24 (2012) 872–881.
[70] F. Valentini, D. Roscioli, M. Carbone, V. Conte, B. Floris, G. Palleschi, R. Flammini, E.M. Bauer, G. Nasillo, E. Caponetti, Anal. Chem. 84 (2012) 5823–5831.
[71] F. Valentini, E. Ciambella, V. Conte, L. Sabatini, N. Ditaranto, F. Cataldo, G. Palleschi, M. Bonchio, F. Giacalone, Z. Syrgiannis, M. Prato, Biosens. Bioelectron. 59 (2014) 94–98.